HHS Public Access

Author manuscript

J Phys Chem B. Author manuscript; available in PMC 2021 February 13.

Published in final edited form as:

J Phys Chem B. 2020 February 13; 124(6): 1065–1070. doi:10.1021/acs.jpcb.9b10987.

NMR Observation of Intermolecular Hydrogen Bonds between Protein Tyrosine Side-Chain OH and DNA Phosphate Groups

Binhan Yu, **Channing C. Pletka**, **Junji Iwahara***

Department of Biochemistry & Molecular Biology, Sealy Center for Structural Biology & Molecular Biophysics, University of Texas Medical Branch, Galveston, Texas 77555-1068, USA

Abstract

Hydrogen bonds between protein side-chain hydroxyl (OH) and phosphate groups are one of the most common types of intermolecular hydrogen bonds in protein-DNA/RNA complexes. Using NMR spectroscopy, we identified and characterized the hydrogen bonds between tyrosine side-chain OH and DNA phosphate groups in a protein-DNA complex. These OH groups exhibited relatively slow hydrogen exchange rates and sizable scalar couplings between hydroxyl ^{1}H and DNA phosphate ^{31}P nuclei across the hydrogen bonds. Information about intermolecular hydrogen bonds facilitates investigations of DNA/RNA recognition by the protein.

Graphical Abstract

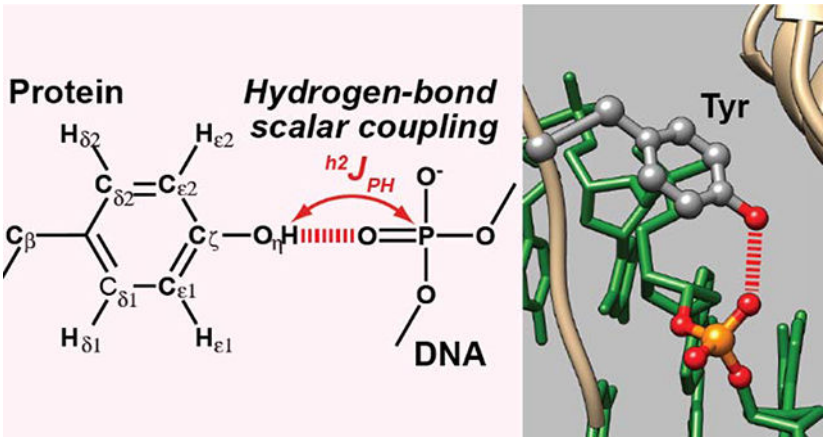

Introduction

Hydrogen bonding is vital for structures and functions of biological molecules.[1] Specific patterns of hydrogen bonds define secondary structures of proteins and nucleic acids. Molecular recognition and catalysis by these molecules are often facilitated through stable or transient intermolecular hydrogen bonds. Therefore, for a mechanistic understanding of a particular biomolecular process, it is important to identify and characterize the hydrogen bonds directly involved in the process.

*To whom correspondence should be addressed. j.iwahara@utmb.edu [Phone] 1-409-747-1403.

NMR spectroscopy is a powerful tool for investigations of hydrogen bonds.[2] Although hydrogen bonds are typically identified using the geometrical criteria of donor and acceptor groups in three-dimensional structures, some NMR methods allow direct identification of hydrogen bonds even without any structural information.[3] These methods became available in the late 90s when scalar couplings across hydrogen bonds (referred to as "hydrogen-bond scalar couplings") were discovered for nucleic-acid base pairs and protein secondary structures.[4–7] Since then, various types of hydrogen-bond scalar couplings have been identified.[8] Hydrogen-bond scalar couplings provide not only structural information but also information about dynamics because these couplings are influenced by the transient distortion or breakage of the hydrogen bonds as well.[9–12]

Observation of intermolecular hydrogen-bond scalar couplings is often more challenging than that of intramolecular hydrogen-bond scalar couplings because self-decoupling occurs when the residence time of the complex is not sufficiently long.[12] Nonetheless, intermolecular hydrogen-bond scalar couplings have been observed for nucleic acids (as reviewed in refs[13–14]), protein–nucleic acid complexes,[12,15–22] and other protein–ligand complexes[23–24]. Observations of intermolecular hydrogen-bond scalar couplings have been made for some protein side chains, including serine (Ser),[23] threonine (Thr),[23] arginine (Arg),[25] histidine (His),[21] and lysine (Lys).[12,15–20]

Another signature of hydrogen bonds detectable by NMR is slow hydrogen exchange.[26] Labile hydrogen atoms of $NH/NH_2/NH_3^+$ or OH groups undergo hydrogen exchange with water. When these groups form stable hydrogen bonds, the hydrogen exchange is generally slower.[27] For example, although ^1H signals of Lys side-chain NH_3^+ groups are typically undetectable due to rapid hydrogen exchange, their ^1H signals are detectable when these moieties interact with other moieties and form hydrogen bonds.[28]

In this work, we used NMR spectroscopy to identify and characterize intermolecular hydrogen bonds between tyrosine (Tyr) side-chain hydroxyl (OH) groups and DNA phosphates in a protein-DNA complex. Although rapid hydrogen exchange often broadens ^1H resonances of OH groups beyond detection, two interfacial Tyr OH groups in contact with DNA phosphates in the fruit-fly Antennapedia homeodomain (Antp HD)–DNA complex exhibited clearly observable ^1H resonances, owing to relatively slow hydrogen exchange. For these OH groups, we were able to observe hydrogen-bond scalar couplings ($^{h2}J_{HP}$) between Tyr side-chain hydroxyl ^1H and DNA phosphate ^{31}P nuclei. Because hydrogen bonds between OH and phosphate groups are highly common in protein-DNA and protein-RNA complexes, NMR data on these hydrogen bonds would be useful for a physicochemical understanding of how proteins recognize nucleic acids.

Experimental Methods

Preparation of the Antp HD–DNA complex

The Antp HD–DNA complex was prepared as previously described.[29] The protein was the 60-residue construct used in the crystallographic study by Pabo and coworkers,[30] rather than the 68-residue construct used in the NMR studies by Wüthrich and coworkers.[31–32] The DNA was the 15-bp DNA with the same sequence as that used for the crystallographic study.

[30] A 370-μl solution of 1.1 mM complex of ^{13}C,^{15}N-lableled Antp HD and unlabeled 15-bp DNA in a pH 5.8 buffer containing 20 mM potassium succinate-d_4, 100 mM KCl, and 0.4 mM NaF (as a preservative) was sealed into a 5-mm coaxial NMR tube (Norell, Inc.). A 2-mm stem insert (Norell, Inc.) containing 100 μl of D_2O was used for the NMR lock.

Through-bond ^{1}H-^{13}C correlation for Tyr side chains

^{1}H, ^{13}C, and ^{15}N resonances of backbone and non-aromatic side chains of the Antp HD–DNA complex used for the current sample had previously been assigned.[20,29] Aromatic ^{13}C-^{1}H resonances were assigned using through-bond correlation signals in a three-dimensional (3D) HCCH-COSY spectrum, two-dimensional (2D) ^{1}H-^{13}C HSQC and (HB)CB(CGCD)HD spectra[33–34] recorded using Bruker Avance III spectrometers equipped with a TCI cryogenic probe at a ^{1}H frequency of 750 or 800 MHz. A long-range HMQC spectrum was recorded to observe hydroxyl $^{1}H_{\eta}$–$^{13}C_{\varepsilon}$ correlation signals via $^{3}J_{CH}$ couplings.

Measurements of hydrogen exchange rates for Tyr OH groups

For the Tyr OH groups, hydrogen exchange rates (k_{HX}) were measured at 15°C and 25°C through one-dimensional (1D) CLEANEX-PM experiments[35] in which a ^{15}N-filter scheme[36] was implemented to exclude signals from NH protons. This ^{15}N filter was incorporated into the WATERGATE scheme[37] in the manner presented in Figure 1D of Ikura and Bax.[36] The experiments were performed at a ^{1}H frequency of 600 MHz using 7 mixing-time points: 0.4, 2.1, 4.2, 8.4, 14.7, 21.0, 33.6, and 62.9 ms. The k_{HX} rates were determined through fitting calculations with Eq. 1 in Hwang et al.[38] using MATLAB (MathWorks, Inc.). Each k_{HX} measurement took ~14 hours with 3744 scans per free induction decay (FID). Uncertainties in the k_{HX} rates were estimated from three replicates.

Observation of hydrogen-bond scalar couplings between Tyr OH and DNA phosphate groups

Hydrogen-bond scalar couplings ($^{h2}J_{HP}$) between Tyr side-chain hydroxyl ^{1}H and DNA ^{31}P nuclei were measured at 15°C using a Bruker Avance III spectrometer equipped with a ^{1}H/^{13}C/^{15}N/^{31}P QCI cryogenic probe operated at a ^{1}H frequency of 600 MHz. To observe ^{1}H-^{31}P correlation signals arising from coherence transfer via $^{h2}J_{HP}$ couplings, a long-range ^{1}H-^{31}P HMQC spectrum was recorded at 15°C with ^{15}N GARP and ^{31}P WALTZ16 decoupling schemes, essentially as previously described.[21] However, a shorter delay for ^{1}H-^{31}P coherence transfer (i.e., 10 ms between ^{1}H and ^{31}P 90° pulses) was used to mitigate the relaxation loss due to rapid hydrogen exchange of the Tyr OH groups. The total experiment time for recording of the ^{1}H-^{31}P HMQC spectrum was ~136 hours. The magnitude of each $^{h2}J_{HP}$ coupling between OH and phosphate groups was measured using a 1D version of the ^{1}H spin-echo $^{h2}J_{HP}$ modulation difference experiment[21] that incorporate a ^{15}N filter scheme involving two 90° ^{15}N pulses separated by $(2J_{NH})^{-1}$ in the manner of Clore et al.[39] The total length of the spin-echo scheme (T_{SE}) was set to 33.6 ms, which was ~3-fold longer than the apparent transverse relaxation time of each OH proton. The absolute value of the coupling constant, $|^{h2}J_{HP}|$, was determined with the following equation: $I_a/I_b = \cos(\pi J T_{SE})$; where I_a and I_b represent the signal intensities in the spectra with and without the $^{h2}J_{HP}$ modulation, respectively. Uncertainties in $|^{h2}J_{HP}|$ were estimated from 3 replicates.

For each, the total measurement time was ~42 hours. Other details about the $|^{h2}J_{HP}|$ measurements are given below.

Statistical analysis of protein side-chain OH–DNA phosphate hydrogen bonds

In total, 3213 crystal structures of protein-DNA or protein-RNA complexes solved at a resolution < 2.5 Å were retrieved from the Research Collaboratory for Structural Bioinformatics (RCSB) PDB server.[40] Using MATLAB, intermolecular hydrogen bonds involving $O_{5'}$, O_{P1}, O_{P2}, or $O_{3'}$ atoms of DNA/RNA phosphate groups were identified using a criterion of O/N…O distance < 3.2 Å. Intermolecular hydrogen bonds between phosphate and Arg guanidium, Lys NH_3^+, Asn/Gln NH_2, or Ser/Thr/Tyr OH groups were counted for the protein-DNA and protein-RNA complexes.

Results

NMR signals from Tyr OH groups

We noticed ^{1}H NMR signals from Tyr OH groups when we analyzed a 3D ^{13}C-edited NOESY-HSQC spectrum recorded for aromatic side chains of the Antp HD–DNA complex. The $^1H_\varepsilon$ nuclei of Tyr8 and Tyr25 exhibited relatively strong cross peaks of the nuclear Overhauser effect (NOE) with ^{1}H resonances at 9.67 and 9.94 ppm, respectively, which did not match with any assigned resonances of ^{13}C- or ^{15}N-attached ^{1}H nuclei within a short (< 4 Å) distance from the Tyr side chains. These ^{1}H resonances were observed in the 1D ^{1}H spectrum as well (Figure 1A). Since 1D ^{1}H spectra with and without ^{15}N (or ^{13}C) decoupling showed these ^{1}H resonances as singlet peaks, these resonances are not from ^{1}H atoms bonded to ^{15}N or ^{13}C. To test the possibility that these ^{1}H resonances are from Tyr OH groups, we recorded a long-range ^{1}H-^{13}C HMQC spectrum using relatively long (10 ms) delays for ^{1}H-^{13}C coherence transfer. If these ^{1}H resonances are from Tyr OH groups, the three-bond scalar couplings ($^3J_{CH}$) between the hydroxyl ^{1}H and aromatic $^{13}C_\varepsilon$ nuclei could be sizable (~5–7 Hz)[41–42]. The obtained spectrum showed cross peaks between these ^{1}H resonances and the $^{13}C_\varepsilon$ resonances of Tyr8 and Tyr25 (Figure 1B–C), which unequivocally indicate that the ^{1}H signals at 9.67 ppm and 9.94 ppm are from the OH groups of Tyr8 and Tyr25, respectively.

Hydrogen exchange of interfacial Tyr OH groups

In the crystal structure of the Antp HD–DNA complex, the OH groups of Tyr8 and Tyr25 formed hydrogen bonds to DNA phosphate groups (Figure 1D). The intermolecular hydrogen bonds explain why these OH groups clearly exhibit ^{1}H resonances although hydroxyl ^{1}H resonances are typically undetectable due to severe broadening caused by rapid hydrogen exchange.[26] In fact, the Antp HD in the free state did not exhibit detectable ^{1}H signals from the Tyr OH groups. To quantitatively assess the hydrogen exchange of the Tyr8 and Tyr25 OH groups, we performed a 1D CLEANEX-PM experiment[35], in which water magnetization was transferred to the OH groups through hydrogen exchange. Since the ^{1}H resonances of the Tyr OH groups were close to some protein NH resonances (in particular, Arg52 $^1H_\varepsilon$ and Trp56 $^1H_{\varepsilon 1}$ resonances; see Figure 1A), we incorporated a ^{15}N filter scheme[33] to suppress the NH resonances. Figure 2A shows intensities of the ^{1}H signals from Tyr 8 and Tyr25 as a function of the mixing time for the transfer. Through nonlinear least-

squares fitting to these data, we determined the hydrogen exchange rates k_{HX} for Tyr8 and Tyr25 OH groups. Figure 2B shows the best-fit curves with the determined values of k_{HX} rates. Interestingly, the hydrogen exchange of the Tyr25 OH group was ~50–100-fold faster than that of the Tyr8 OH group. The rapid hydrogen exchange of the Tyr25 OH group is consistent with its broader ^{1}H resonance (see Figure 1A–B). The crystal structure and hydrogen-bond scalar couplings in solution (see below) suggest that the hydrogen-bonding geometry is similar for these two Tyr OH groups. However, the Tyr8 OH group is more buried in the binding interface and its solvent accessible surface areas is remarkably smaller (Figure 2C). Therefore, the slower hydrogen exchange rate of the Tyr8 OH group could be due to less accessibility for water.

Direct evidence of Tyr OH–phosphate hydrogen bonds

To examine whether the interfacial Tyr OH groups in contact with DNA phosphates exhibit hydrogen-bond scalar couplings $^{h2}J_{HP}$, we recorded a long-range ^{1}H-^{31}P HMQC spectrum. As shown in Figure 3A, this spectrum clearly showed ^{1}H-^{31}P correlation signals arising from coherence transfer via $^{h2}J_{HP}$ couplings for the Tyr8 and Tyr25 OH groups. Compared to typical ^{31}P chemical shifts of B-form DNA (−4.6 to −4.0 ppm with respect to tetramethyl phosphate [TMP]),[43] the ^{31}P chemical shifts of these signals were up-field shifted presumably due to the hydrogen bonds. This shift was also clearly observed in 1D ^{31}P spectrum recorded for the sample (Figure 3B). Through the 1D spin-echo $^{h2}J_{HP}$ modulation difference experiment, we also measured the magnitude of the $^{h2}J_{HP}$ couplings. In this experiment, ^{15}N-filtered 1D ^{1}H spectra were recorded after the spin-echo period with and without $^{h2}J_{HP}$ modulation (Figure 3C). The values of $|^{h2}J_{HP}|$ for the OH groups of Tyr8 and Tyr25 were determined to be 3.0 ± 0.1 and 3.4 ± 0.3 Hz, respectively. These couplings were significantly larger compared to those between the Ser/Thr hydroxyl ^{1}H and FMN ^{31}P nuclei in the flavodoxin-FMN complex (0.5 – 1.7 Hz)[23] despite similar O···O distances (2.53 – 2.87 Å for Tyr and 2.49 – 2.79 Å for Ser/Thr) in the crystal structures. Although the hydrogen bonds may differ in the positionings of hydrogen atoms of the rotatable OH groups, this possibility cannot be examined in the current case because the crystal structures do not include hydrogen atomic coordinates. Nonetheless, the observed $^{h2}J_{HP}$ couplings represent direct evidence of the intermolecular hydrogen bonds in solution.

Discussion

In this study, we observed the hydrogen-bond scalar couplings between the Tyr OH and DNA phosphate groups in the Antp HD–DNA complex. Although rapid hydrogen exchange typically precludes observation of hydroxyl ^{1}H resonances,[26] some OH groups of protein side chains and RNA nucleotides have been observed around 5.5–12.4 ppm in previous studies.[23,41–42,44–48] For example, Löhr et al. observed hydrogen-bond scalar couplings between hydroxyl ^{1}H and FMN ^{31}P nuclei for two Ser and two Thr OH groups in the flavodoxin-FMN complex.[23] Thus, measurements of hydrogen-bond scalar couplings are feasible for some OH groups.

Given this feasibility, statistical information about hydrogen bonding between protein side-chain OH and DNA/RNA phosphate groups may be of practical interest for researchers who

study protein-DNA or protein-RNA complexes. A statistic study published in 2001 by Luscombe et al.[49] suggested that hydrogen bonds between protein side-chain OH and DNA phosphate groups are common among protein-DNA complexes. However, the total number of structures of protein-DNA complexes was far less at that time. Therefore, using the currently available 3213 crystal structures of protein-DNA or protein-RNA complexes solved at a resolution < 2.5 Å, we updated the statistics of intermolecular hydrogen bonds involving phosphate groups.

Table 1 show the frequencies of these intermolecular hydrogen bonds in the crystal structures of protein-DNA/RNA complexes. The statistical data confirmed that protein side-chain OH groups are one of the most common hydrogen bond donors to phosphate groups. Interestingly, although OH groups are not charged, the hydrogen bonds between OH and phosphate groups are even more common than those of NH_3^+-phosphate ion pairs in protein-DNA complexes. On average, there are 2–3 hydrogen bonds between protein side-chain OH and phosphate groups per structure of protein-nucleic acid complex. Thus, hydrogen-bond scalar couplings between protein hydroxyl ^1H and phosphate ^{31}P nuclei would be useful for structural and dynamic investigations of protein-DNA/RNA complexes.

As previously noted,[8] hydrogen-bond scalar couplings are sensitive to a subtle difference in hydrogen-bonding geometry. Because OH groups are rotatable, their $^{h2}J_{HP}$ couplings should also depend on the bond rotation dynamics. Although these characteristics may cause difficulty in quantitative interpretation of $^{h2}J_{HP}$ couplings for OH groups, molecular dynamics simulations might facilitate interpretation of hydrogen-bond scalar couplings.

Conclusions

We demonstrated an NMR-based identification and characterization of the intermolecular hydrogen bonds between protein side-chain OH and DNA phosphate groups. The interfacial Tyr OH groups exhibited sizable $^{h2}J_{HP}$ couplings across the hydrogen bonds. These Tyr OH groups showed relatively slow hydrogen exchange rates as measured by the CLEANEX-PM method. These Tyr OH groups also exhibited NOE cross peaks with some being intermolecular NOEs (data not shown). Most likely, the same approach would be applicable to protein-RNA complexes as well. Because intermolecular hydrogen bonds between protein side-chain OH and nucleic-acid phosphate groups are common in protein-DNA/RNA complexes, we expect that the NMR-based investigations of this type of hydrogen bonds would facilitate biophysical investigations of many protein-nucleic acid complexes.

Acknowledgments

This work was supported by Grant R35-GM130326 from the National Institutes of Health (to J.I.). We thank Dr. Tianzhi Wang for maintenance of the NMR equipment at University of Texas Medical Branch.

References

1. Fersht AR, Structure and mechanism in protein science: a guide to enzyme catalysis and protein folding. W. H. Freeman: New York, 1998.
2. Dingley AJ; Cordier F; Grzesiek S, An introduction to hydrogen bond scalar couplings. Concepts Magn. Reson. 2001, 13, 103–127.

3. Arunan E; Desiraju GR; Klein RA; Sadlej J; Scheiner S; Alkorta I; Clary DC; Crabtree RH; Dannenberg JJ; Hobza P, et al., Definition of the hydrogen bond (IUPAC recommendations 2011). Pure Appl. Chem. 2011, 83, 1611–1636.
4. Cordier F; Grzesiek S, Direct observation of hydrogen bonds in proteins by interresidue $^{3h}J_{NC'}$ scalar couplings. J. Am. Chem. Soc. 1999, 121, 1601–1602.
5. Cornilescu G; Hu JS; Bax A, Identification of the hydrogen bonding network in a protein by scalar couplings. J. Am. Chem. Soc. 1999, 121, 2949–2950.
6. Dingley AJ; Grzesiek S, Direct observation of hydrogen bonds in nucleic acid base pairs by internucleotide $^{2}J_{NN}$ couplings. J. Am. Chem. Soc. 1998, 120, 8293–8297.
7. Pervushin K; Ono A; Fernandez C; Szyperski T; Kainosho M; Wüthrich K, NMR scalar couplings across Watson-Crick base pair hydrogen bonds in DNA observed by transverse relaxation-optimized spectroscopy. Proc. Natl. Acad. Sci. U. S. A. 1998, 95, 14147–14151. [PubMed: 9826668]
8. Grzesiek S; Cordier F; Jaravine V; Barfield M, Insights into biomolecular hydrogen bonds from hydrogen bond scalar couplings. Prog. NMR Spect. 2004, 45, 275–300.
9. Jaravine VA; Alexandrescu AT; Grzesiek S, Observation of the closing of individual hydrogen bonds during TFE-induced helix formation in a peptide. Protein Sci. 2001, 10, 943–950. [PubMed: 11316874]
10. Markwick PR; Sprangers R; Sattler M, Dynamic effects on *J*-couplings across hydrogen bonds in proteins. J. Am. Chem. Soc. 2003, 125, 644–645. [PubMed: 12526659]
11. Zandarashvili L; Li DW; Wang T; Brüschweiler R; Iwahara J, Signature of mobile hydrogen bonding of lysine side chains from long-range ^{15}N-^{13}C scalar *J*-couplings and computation. J. Am. Chem. Soc. 2011, 133, 9192–9195. [PubMed: 21591797]
12. Zandarashvili L; Esadze A; Kemme CA; Chattopadhyay A; Nguyen D; Iwahara J, Residence times of molecular complexes in solution from NMR data of intermolecular hydrogen-bond scalar coupling. J. Phys. Chem. Lett. 2016, 7, 820–824. [PubMed: 26881297]
13. Dallmann A; Sattler M, Detection of hydrogen bonds in dynamic regions of RNA by NMR spectroscopy. Curr. Protoc. Nucleic Acid. Chem. 2014, 59, 7 22 21–27 22 19.
14. Majumdar A; Patel DJ, Identifying hydrogen bond alignments in multistranded DNA architectures by NMR. Acc. Chem. Res. 2002, 35, 1–11. [PubMed: 11790083]
15. Anderson KM; Esadze A; Manoharan M; Brüschweiler R; Gorenstein DG; Iwahara J, Direct observation of the ion-pair dynamics at a protein-DNA interface by NMR spectroscopy. J. Am. Chem. Soc. 2013, 135, 3613–3619. [PubMed: 23406569]
16. Anderson KM; Nguyen D; Esadze A; Zandrashvili L; Gorenstein DG; Iwahara J, A chemical approach for site-specific identification of NMR signals from protein side-chain NH3+ groups forming intermolecular ion pairs in protein-nucleic acid complexes. J. Biomol. NMR 2015, 62, 1–5. [PubMed: 25690740]
17. Chen CY; Esadze A; Zandarashvili L; Nguyen D; Pettitt BM; Iwahara J, Dynamic equilibria of short-range electrostatic interactions at molecular interfaces of protein-DNA complexes. J. Phys. Chem. Lett. 2015, 6, 2733–2737. [PubMed: 26207171]
18. Esadze A; Chen C; Zandarashvili L; Roy S; Pettitt BM; Iwahara J, Changes in conformational dynamics of basic side chains upon protein-DNA association. Nucleic Acids Res. 2016, 44, 6961–6970. [PubMed: 27288446]
19. Zandarashvili L; Esadze A; Vuzman D; Kemme CA; Levy Y; Iwahara J, Balancing between affinity and speed in target DNA search by zinc-finger proteins via modulation of dynamic conformational ensemble. Proc. Natl. Acad. Sci. U. S. A. 2015, 112, E5142–5149. [PubMed: 26324943]
20. Zandarashvili L; Nguyen D; Anderson KM; White MA; Gorenstein DG; Iwahara J, Entropic enhancement of protein-DNA affinity by oxygen-to-sulfur substitution in DNA phosphate. Biophys. J. 2015, 109, 1026–1037. [PubMed: 26331260]
21. Chattopadhyay A; Esadze A; Roy S; Iwahara J, NMR scalar couplings across intermolecular hydrogen bonds between zinc-finger histidine side chains and DNA phosphate groups. J. Phys. Chem. B 2016, 120, 10679–10685. [PubMed: 27685459]

22. Liu AZ; Majumdar A; Jiang F; Chernichenko N; Skripkin E; Patel DJ, NMR detection of intermolecular N-H•••N hydrogen bonds in the human T cell leukemia virus-1 Rex peptide-RNA aptamer complex. J. Am. Chem. Soc. 2000, 122, 11226–11227.
23. Löhr F; Mayhew SG; Rüterjans H, Detection of scalar couplings across NH···OP and OH···OP hydrogen bonds in a flavoprotein. J. Am. Chem. Soc. 2000, 122, 9289–9295.
24. Mishima M; Hatanaka M; Yokoyama S; Ikegami T; Walchli M; Ito Y; Shirakawa M, Intermolecular ^{31}P-^{15}N and ^{31}P-^{1}H scalar couplings across hydrogen bonds formed between a protein and a nucleotide. J. Am. Chem. Soc. 2000, 122, 5883–5884.
25. Liu A; Hu W; Majumdar A; Rosen MK; Patel DJ, NMR detection of side chain-side chain hydrogen bonding interactions in ^{13}C/^{15}N-labeled proteins. J. Biomol. NMR 2000, 17, 305–310. [PubMed: 11014594]
26. Wüthrich K, NMR of proteins and nucleic acids. Wiley-Interscience: New York, 1986.
27. Englander SW; Downer NW; Teitelbaum H, Hydrogen exchange. Annu. Rev. Biochem. 1972, 41, 903–924. [PubMed: 4563445]
28. Nguyen D; Chen C; Pettitt BM; Iwahara J, NMR Methods for characterizing the basic side chains of proteins: electrostatic interactions, hydrogen bonds, and conformational dynamics. Methods Enzymol. 2019, 615, 285–332. [PubMed: 30638532]
29. Nguyen D; Hoffpauir ZA; Iwahara J, Internal motions of basic side chains of the Antennapedia homeodomain in the free and DNA-bound states. Biochemistry 2017, 56, 5866–5869. [PubMed: 29045141]
30. Fraenkel E; Pabo CO, Comparison of X-ray and NMR structures for the Antennapedia homeodomain-DNA complex. Nat. Struct. Biol. 1998, 5, 692–697. [PubMed: 9699632]
31. Otting G; Qian YQ; Billeter M; Muller M; Affolter M; Gehring WJ; Wüthrich K, Protein-DNA contacts in the structure of a homeodomain-DNA complex determined by nuclear magnetic resonance spectroscopy in solution. EMBO J. 1990, 9, 3085–3092. [PubMed: 1976507]
32. Qian YQ; Billeter M; Otting G; Muller M; Gehring WJ; Wüthrich K, The structure of the Antennapedia homeodomain determined by NMR spectroscopy in solution: comparison with prokaryotic repressors. Cell 1989, 59, 573–580. [PubMed: 2572329]
33. Cavanagh J; Fairbrother WJ; Palmer AG III; Rance M; Skelton NJ, Protein NMR sprectroscopy: principles and practice. 2 ed.; Elsevier Academic Press: Burlignton, 2007.
34. Yamazaki T; Forman-Kay JD; Kay LE, Two-Dimensional NMR Experiments for correlating ^{13}Cβ and ^{1}Hδ/ϵ chemical shifts of aromatic residues in ^{13}C-labeled proteins via scalar couplings. J. Am. Chem. Soc. 1993, 115, 11054–11055.
35. Hwang TL; Mori S; Shaka AJ; Van Zijl PCM, Application of phase-modulated CLEAN chemical EXchange spectroscopy (CLEANEX-PM) to detect water - protein proton exchange and intermolecular NOEs. J. Am. Chem. Soc. 1997, 119, 6203–6204.
36. Ikura M; Bax A, Isotope-filtered 2D NMR of a protein-peptide complex: study of a skeletal muscle myosin light chain kinase fragment bound to calmodulin. J. Am. Chem. Soc. 1992, 114, 2433–2440.
37. Piotto M; Saudek V; Sklenar V, Gradient-tailored excitation for single-quantum NMR spectroscopy of aqueous solutions. J. Biomol. NMR 1992, 2, 661–665. [PubMed: 1490109]
38. Hwang TL; van Zijl PC; Mori S, Accurate quantitation of water-amide proton exchange rates using the phase-modulated CLEAN chemical EXchange (CLEANEX-PM) approach with a Fast-HSQC (FHSQC) detection scheme. J. Biomol. NMR 1998, 11, 221–226. [PubMed: 9679296]
39. Clore GM; Murphy EC; Grogenborn AM; Bax A, Determination of three-bond $^{1}H_{3'}$–^{31}P couplings in nucleic acids and protein-nucleic acid complexes by quantitative *J* correlation spectroscopy. J. Magn. Reson. 1998, 134, 164–167. [PubMed: 9740744]
40. Berman HM; Westbrook J; Feng Z; Gilliland G; Bhat TN; Weissig H; Shindyalov IN; Bourne PE, The Protein Data Bank. Nucleic Acids Res. 2000, 28, 235–242. [PubMed: 10592235]
41. Baturin SJ; Okon M; McIntosh LP, Structure, dynamics, and ionization equilibria of the tyrosine residues in Bacillus circulans xylanase. J. Biomol. NMR 2011, 51, 379–394. [PubMed: 21912982]
42. Werner MH; Clore GM; Fisher CL; Fisher RJ; Trinh L; Shiloach J; Gronenborn AM, Correction of the NMR structure of the ETS1/DNA complex. J. Biomol. NMR 1997, 10, 317–328. [PubMed: 9460239]

43. Gorenstein DG, Conformation and dynamics of DNA and protein-DNA complexes by ^{31}P NMR. Chem. Rev. 1994, 94, 1315–1338.
44. Brockerman JA; Okon M; McIntosh LP, Detection and characterization of serine and threonine hydroxyl protons in Bacillus circulans xylanase by NMR spectroscopy. J. Biomol. NMR 2014, 58, 17–25. [PubMed: 24306180]
45. Fohrer J; Hennig M; Carlomagno T, Influence of the 2'-hydroxyl group conformation on the stability of A-form helices in RNA. J. Mol. Biol. 2006, 356, 280–287. [PubMed: 16376377]
46. Hennig M; Fohrer J; Carlomagno T, Assignment and NOE analysis of 2'-hydroxyl protons in RNA: implications for stabilization of RNA A-form duplexes. J. Am. Chem. Soc. 2005, 127, 2028–2029. [PubMed: 15713064]
47. Liepinsh E; Otting G; Wüthrich K, NMR spectroscopy of hydroxyl protons in aqueous solutions of peptides and proteins. J. Biomol. NMR 1992, 2, 447–465. [PubMed: 1384851]
48. Ying J; Bax A, 2'-hydroxyl proton positions in helical RNA from simultaneously measured heteronuclear scalar couplings and NOEs. J. Am. Chem. Soc. 2006, 128, 8372–8373. [PubMed: 16802782]
49. Luscombe NM; Laskowski RA; Thornton JM, Amino acid-base interactions: a three-dimensional analysis of protein-DNA interactions at an atomic level. Nucleic Acids Res. 2001, 29, 2860–2874. [PubMed: 11433033]

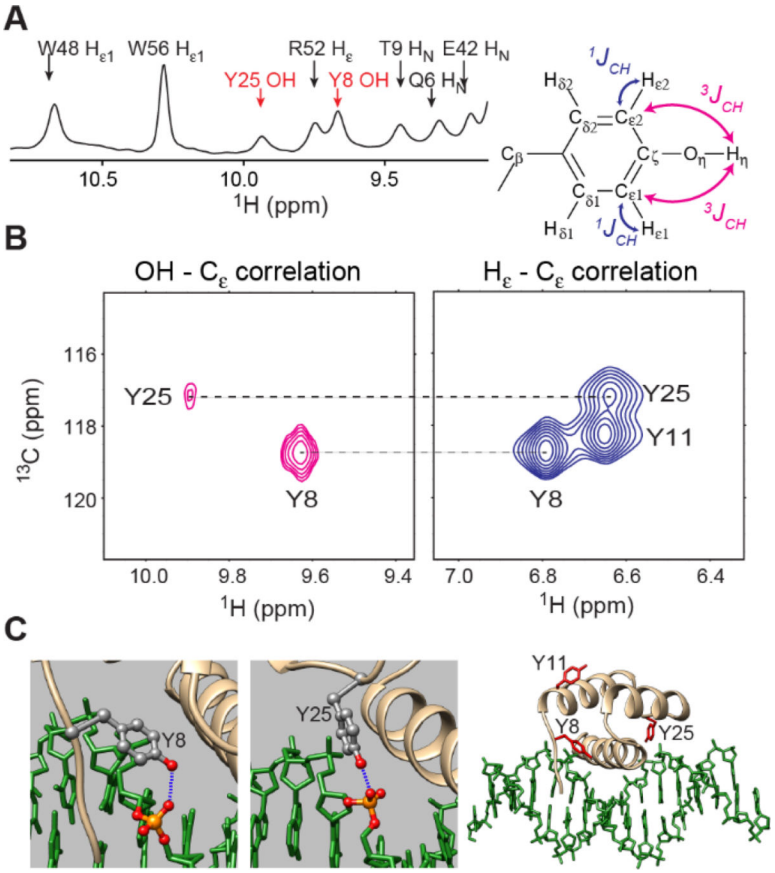

Figure 1.

NMR signals from Y8 and Y25 OH groups at the protein-DNA interface of the complex of $^{13}C,^{15}N$-labeled Antp HD and unlabeled 15-bp DNA at 15˚C. (**A**) The Tyr OH signals in a 1D ^{1}H spectrum recorded with ^{15}N decoupling. (**B**) Through-bond correlations between Tyr hydroxyl ^{1}H and $^{13}C_{\varepsilon}$ nuclei observed in a long-range ^{1}H-^{13}C HMQC spectrum. $^{1}H_{\varepsilon}$–$^{13}C_{\varepsilon}$ correlations observed in a standard ^{1}H-^{13}C HMQC spectrum recorded for the same complex is also shown. (**C**) Interactions between Tyr side-chain OH and DNA phosphate groups in the 2.5-Å resolution crystal structure of the Antp HD–DNA complex (PDB 9ANT)[30].

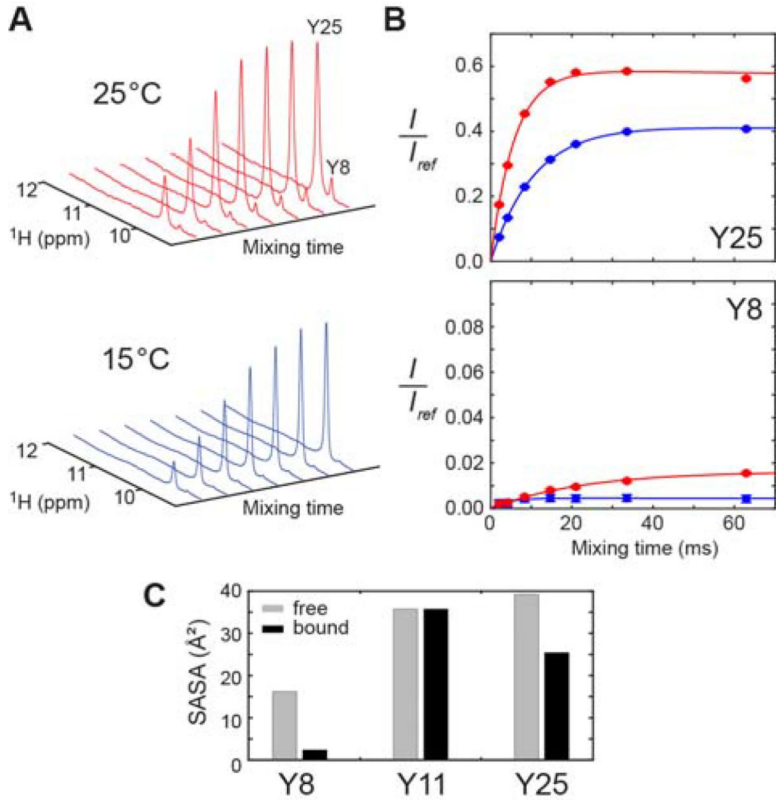

Figure 2.

Hydrogen exchange of the interfacial Tyr OH groups of the Antp HD–DNA complex. (**A**) Series of 1D ^{1}H spectra recorded in the ^{15}N-filtered CLEANEX-PM experiment for the complex of ^{15}N-lableled Antp HD and 15-bp DNA. (**B**) CLEANEX-PM data for determination of the hydrogen exchange rates k_{HX} for Y8 and Y25 OH groups in the Antp HD–DNA complex at 25°C (red) and 15°C (blue). The ratio of the signal intensity observed in the CLEANEX-PM experiment to the signal intensity in the reference spectrum is plotted for each mixing time.[35] The solid lines represent best-fit curves obtained through fitting as described by Hwang et al.[38] The k_{HX} rate for the Tyr25 OH group was 43 ± 3 s^{-1} at 15°C and 106 ± 4 s^{-1} at 25°C. The k_{HX} rate for the Tyr8 OH group was determined to be 0.74 ± 0.04 s^{-1} at 25°C and 1.1 ± 0.6 s^{-1} at 15°C. (**C**) Solvent accessible surface areas of the Tyr O_{η} atoms in the crystal structure (PDB 9ANT).

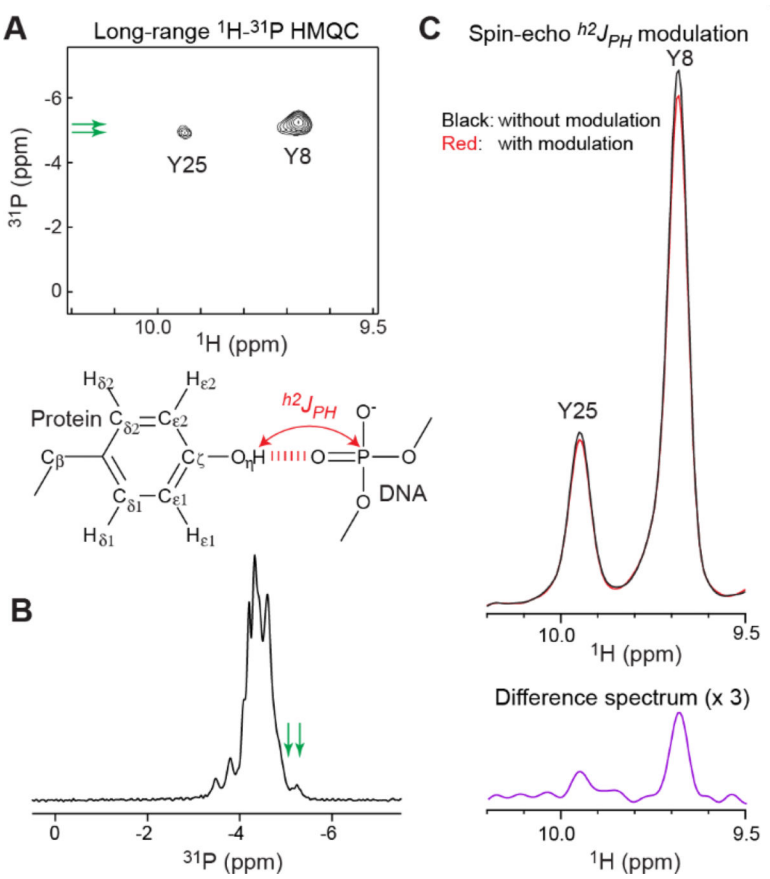

Figure 3.

Observation of hydrogen-bond scalar couplings $^{h2}J_{PH}$ between DNA phosphate ^{31}P and Tyr hydroxyl ^{1}H nuclei for the Antp HD–DNA complex. (**A**) 2D long-range ^{1}H-^{31}P HMQC spectrum. ^{1}H-^{31}P correlation signals arising from coherence transfer via $^{h2}J_{PH}$ couplings were observed for the Tyr8 and Tyr25 OH groups. ^{31}P chemical shifts are with respect to TMP. (**B**) 1D ^{31}P spectrum recorded for the same complex. The positions of the ^{31}P resonances observed in the long-range ^{1}H-^{31}P HMQC are indicated by green arrow. (**C**) Data of 1D spin-echo $^{h2}J_{PH}$ modulation difference experiment incorporating a ^{15}N filter scheme. The signals from the Y8 and Y25 OH groups in the subspectra recorded with and without $^{h2}J_{PH}$ modulation and a difference spectrum are shown. From these data, the values of $|\,^{h2}J_{PH}\,|$ for the Y8 and Y25 OH groups were determined to be 3.0 ± 0.1 and 3.4 ± 0.3 Hz, respectively.

Table 1

Statistics of intermolecular hydrogen bonds of phosphate groups in PDB crystal structures of protein-nucleic acids complexes.

Protein-DNA complexes:		2607 [a)]
Donor	Acceptor	Hydrogen bonds [b)]
Arg guanidium	Phosphate	7629
Lys NH_3^+	Phosphate	3618
Asn/Gln NH_2	Phosphate	1929 (1127/802) [c)]
Ser/Thr/Tyr OH	Phosphate	6475 (2399/2590/1486) [c)]
Protein-RNA complexes:		606 [a)]
Donor	Acceptor	Hydrogen bonds [b)]
Arg guanidium	Phosphate	6702
Lys NH_3^+	Phosphate	3065
Asn/Gln NH_2	Phosphate	1016 (613/403) [c)]
Ser/Thr/Tyr OH	Phosphate	2219 (902/753/564) [c)]

[a)] Total number of crystal structures with a resolution < 2.5 Å.

[b)] Total number of hydrogen bonds identified using a criterion of the N/O…O distance < 3.2 Å.

[c)] Numbers in parentheses indicate data for individual types of side chains.